HHS Public Access

Author manuscript

J Am Chem Soc. Author manuscript; available in PMC 2021 June 10.

Published in final edited form as:

J Am Chem Soc. 2020 June 10; 142(23): 10325–10330. doi:10.1021/jacs.0c04422.

Homobenzylic Oxygenation Enabled by Dual Organic Photoredox and Cobalt Catalysis

Joshua B. McManus[‡],
Department of Chemistry, University of North Carolina at Chapel Hill, Chapel Hill, North Carolina 27599-3290, United States

Jeremy D. Griffin[‡],
Department of Chemistry, University of North Carolina at Chapel Hill, Chapel Hill, North Carolina 27599-3290, United States

Alexander R. White,
Department of Chemistry, University of North Carolina at Chapel Hill, Chapel Hill, North Carolina 27599-3290, United States

David A. Nicewicz
Department of Chemistry, University of North Carolina at Chapel Hill, Chapel Hill, North Carolina 27599-3290, United States

Abstract

Activation of aliphatic C(sp^3)–H bonds in the presence of more activated benzylic C(sp^3)–H bonds is often a nontrivial, if not impossible task. Herein we show that leveraging the reactivity of benzylic C(sp^3)–H bonds to achieve reactivity at the homobenzylic position can be accomplished using dual organic photoredox/cobalt catalysis. Through a two-part catalytic system, alkyl arenes undergo dehydrogenation followed by an anti-Markovnikov Wacker-type oxidation to grant benzyl ketone products. This formal homobenzylic oxidation is accomplished with high atom economy without the use of directing groups, achieving valuable reactivity that traditionally would require multiple chemical transformations.

Selective chemical modification of unactivated aliphatic C–H bonds represents a tremendous challenge in organic chemistry.[1] Nature routinely utilizes biosynthetic enzymes to selectively oxygenate specific C–H bonds with high substrate fidelity.[2] While such selectivity is highly coveted, chemists have struggled to mimic nature's adept ability for site-selective oxidation of hydrocarbon scaffolds.

Corresponding Author: **David A. Nicewicz** – *Department of Chemistry, University of North Carolina at Chapel Hill, Chapel Hill, North Carolina 27599-3290, United States;* nicewicz@unc.edu.

[‡]J.B.M. and J.D.G. contributed equally.

Notes

The authors declare no competing financial interest.

Supporting Information

The Supporting Information is available free of charge at https://pubs.acs.org/doi/10.1021/jacs.0c04422.

Experimental procedures and supporting ^1H and ^{13}C NMR spectra (PDF)

Common strategies for effecting selective C–H functionalization target benzylic or allylic C–H bonds, which have low bond-dissociation energies.[3,4] These methods rely on stoichiometric specialty oxidants like IBX (Figure 1A).[5,6] More recently, catalytic methods utilizing transition metals, electro-chemistry, and photoredox chemistry have been developed.[3,7–10] While there are well-established methods for functionalizing activated positions, manipulation of remote C–H bonds remains a challenge.

Conversion of unactivated aliphatic methylenes to ketone-bearing carbons represents a valuable synthetic transformation. Not only does this reactivity paradigm grant access to diverse oxygenated derivatives, but the versatility of ketones allows for streamlined diversification of the resulting products. Curci and co-workers have demonstrated methylene-to-ketone oxidation using super-stoichiometric amounts of highly reactive dioxirane oxidants;[11] however, selectivity is problematic.[12]

Recent work has shown that remote electronics can promote selective C–H functionalization at 2° positions, but only in the absence of reactive benzylic, allylic, or 3° C–H bonds.[13–18] While these methods represent the state-of-the-art for achieving oxidation of unactivated C(sp^3)–H bonds, they largely give modest site-selectivity when multiple similar C–H bonds are present. Differentiation of C–H bonds that are in similar electronic and steric environments requires the use of directing groups that coordinate to transition metals, facilitating reactions with adjacent C–H bonds.[19,20]

Inspired by the dual transition metal/photoredox-catalyzed dehydrogenation protocol developed by Kanai and co-workers,[21,22] we envisioned a selective reaction manifold for methylene oxygenation at the homobenzylic position of saturated alkyl arenes. This strategy would rely on a formal dehydrogenation via the intermediacy of a photoredox-generated benzylic radical (**1˙**) to produce a styrene (**3**) *in situ* (Figure 1C). Hydration followed by a second dehydrogenation would invoke a net anti-Markovnikov Wacker-type oxidation to produce a ketone. The feasibility of this sequence has been demonstrated by Lei and co-workers,[23] and is dependent on the photoredox-catalyzed anti-Markovnikov addition of nucleophiles to alkene radical cations, a topic that has been rigorously studied by our group.[24,25] By the virtue of this mechanism, we were able to achieve an entirely selective oxidation at the homobenzylic position of alkyl arenes. While many C–H functionalization reactions exploit the inherent reactivity of labile benzylic hydrogen atoms, this unique transformation leverages this property to achieve a selective remote oxidation.

Reaction development focused on the transformation of propylbenzene (**1a**) to phenyl-2-propanone (**2a**) (Table 1).[26] To invoke the desired transformation, we devised initial reaction conditions consisting of a hydrogen evolving cobaloxime catalyst and an acridinium photooxidant. Upon irradiation with blue LEDs, quenching of the acridinium excited state by $LiNO_3$ generates a nitrate radical capable of abstracting a benzylic hydrogen atom,[27] initiating the reaction. We investigated cobaloxime complexes judiciously, as they are known to be effective hydrogen-evolving catalysts,[28–30] especially in the presence of organic acids generated by acridinium photooxidants.[21,23] Of the Co catalysts that were explored, the difluoroborate-bridged [Co^{II}] species outperformed [Co^{III}]A–C (Table 1, entries 1–4), although it was only marginally superior to [Co^{III}]A. It was later determined that yields

could be dramatically improved by including a catalytic amount of HNO_3, which is suspected to promote turnover of the cobaloxime (Table 1, entry 5).[29,30]

Reaction progress kinetic analysis (RPKA) has been employed as a tool for studying reaction kinetics. It can be used to gain mechanistic insight and guide the optimization of reactions without the need for multiple pseudo-first-order experiments.[31] Under RPKA conditions (Table 1, entry 5) (initial concentration = 95 mM **1a**) a brief induction period (~20 min) was observed; the reaction then proceeds at a relatively high rate reaching ~15% conversion after 3 h (red trace, Figure 2). However, the reaction quickly tails off and only reaches ~40% after 20 h. These results suggest that conversion may be thwarted by either product inhibition or catalyst decomposition. To probe these possibilities, a same-excess experiment was performed by initiating the reaction at a lower concentration of **1a** while maintaining all other stoichiometric reagents at the same relative concentrations (Figure 2).[26] Though $LiNO_3$ is used in stoichiometric quantities, it was treated as a catalyst as its effective concentration should remain constant. Because this experiment was designed to simulate the reaction at approximately 30% conversion, product **2a** was added in an attempt to rule out product inhibition.

The same-excess experiment revealed a similar reaction profile to that of the standard conditions (Table 1, entry 5); however, when the time axis is offset such that t_0 of the same-excess trial is aligned with the standard experiment where concentrations of **1a** are equal (65 mM), the curves are mismatched (time offset, Figure 2B). Ideally, catalyst concentrations should remain constant throughout; a mismatch indicates that catalyst degradation is probable. The concentration of **2a** should also be equivalent in both reactions at that time point, therefore product inhibition can be ruled out as a cause for diminished consumption of **1a** under standard conditions.

Further optimization included a more extensive survey of acid additives.[26] Dichloroacetic acid (DCA) was identified as a superior additive, giving a significant boost in reproducibiliy, though only delivering modest improvements in yield relative to HNO_3 (Table 1, entry 6). However, increasing the cobaloxime catalyst loading from 5% to 10% furnished reproducibly good yields (Table 1, entries 7 and 8). We believe the implementation of DCA, by acting as a buffer for *in situ*-generated HNO_3, is beneficial for mitigating acid-induced decomposition of the cobaloxime catalyst. These findings are congruent with the results of the same-excess experiment.

Similarly, we recognized that the benzylic protons present on the mesityl group of our most commonly utilized acridinium photocatalyst, **Mes-Acr$^+$**, represented a liability for catalyst decomposition. Unsurprisingly, replacement of the most sterically accessible methyl group with a fluorine atom resulted in increased robustness with a variety of other alkyl arenes. As such, the modified catalyst, **Xyl^F-Acr$^+$** (Chart 1), was implemented to explore the remainder of the substrate scope.

Simple linear alkyl-substituted arenes, such as propyl- and heptylbenzene, were competent substrates in this reaction giving smooth conversion to the desired ketone products **2a** and **2b**, respectively. Modest yields were observed for **2c**, demonstrating that the homobenzylic

position can be oxidized selectively in the presence of 3° benzylic C–H bonds. Interestingly, introducing additional benzylic C–H bonds on the aryl ring did not have a significant effect on reactivity, as **2d** was still formed in good yield. Arenes with useful functional handles—such as bromide—and biphenyl moieties were also competent substrates as demonstrated by **2e** and **2f**, respectively. One potentially synthetically valuable application of this methodology is exemplified by the direct conversion of **1g** to the corresponding β-ketoester **2g**.

We propose that this reaction proceeds through the mechanism outlined in Scheme 1. Initial oxidation of the nitrate anion ($E^{ox}_{p/2} = +1.97V$)[32] occurs from the excited-state photooxidant, **Xyl^F-Acr$^+$*** ($E^*_{red} = +2.13V$).[33] The resulting nitrate radical is a potent H-atom abstracting agent,[27] allowing it to excise the weak C(sp^3)–H bond of **1**, generating HNO_3 and benzylic radical **1$^\bullet$**. **Xyl^F-Acr$^\bullet$** ($E^{ox}_{1/2} = -0.54V$) can feasibly undergo single electron transfer (SET) with [Co^{II}] ($E^{red}_{1/2} = -0.51V$) to regenerate **Xyl^F-Acr$^+$**, and a reduced cobalt complex (*vide infra*). [Co^I]$^-$ likely undergoes protonation to form [Co^{III}]–H assisted by the aforementioned acid additive. **1$^\bullet$** is then intercepted by [Co^{III}]–H, liberating H_2 and **3**. There are several mechanisms by which this could occur:[34–37] One possibility is the direct protonation of [Co^{III}]–H. This would form [Co^{III}]$^+$ ($E^{red}_{1/2} \approx +0.2V$),[28] which could potentially oxidize **1$^\bullet$** ($E^{ox}_{1/2} \approx +0.37V$).[38] While this SET is endergonic by about +0.2 V (4.6 kcal/mol), rapid deprotonation of the resulting benzylic cation intermediate would render SET irreversible, ultimately generating styrene **3**. Alternatively, two molecules of [Co^{III}]–H could undergo a bimolecular reductive elimination of H_2 generating two equivalents of [Co^{II}].[29] **3** would then be formed via the addition of **1$^\bullet$** to [Co^{II}], forming a putative [Co^{III}] alkyl intermediate capable of undergoing a net β-hydride elimination. **3** can then engage in a second catalytic cycle to form the olefin radical cation (**3$^{\bullet+}$**), whereupon trapping with water would afford a distonic radical cation (**2$^{\bullet+}$**). Subsequent deprotonation and a second dehydrogenation would furnish the desired product **2** via a sequence akin to the mechanisms proposed by Lei and Nicewicz.[23,24]

The role of the cobaloxime in this reaction is two-fold: it is responsible for (1) hydrogen evolution and (2) turnover of the photoredox cycle via oxidation of **Xyl^F-Acr$^\bullet$**. The latter was probed using stopped-flow kinetic analysis.[26] Surprisingly, given only a modest driving force for electron transfer, the bimolecular electron transfer between the acridine radical and the Co(II) complex was found to occur during the mixing time of the experiment; thus, only a lower limit estimate of $>10^7$ M^{-1} s^{-1} could be determined for the rate of electron transfer.[26]

Stern–Volmer analysis revealed that both the nitrate anion and β-methylstyrene quench the excited state acridinium on the order of 10^9 M^{-1} s^{-1}, unlike **1a**, which was a poor quencher (Chart 2A). These observations lend credence to the proposed photoinduced electron transfer events outlined in Scheme 1. Interestingly, styrenes were seldom detected in the ^{1}H NMR spectra of crude reaction mixtures. This is likely a result of styrene being the most efficient quencher of **Xyl^F-Acr$^+$*** present in the reaction mixture, with the styrenyl intermediate only existing transiently before rapidly oxidizing to the olefin radical cation. Furthermore,

subjecting **3a** to the reaction conditions produced near-quantitative conversion to **2a**, indicating that styrenes are plausible intermediates.

Having established a working mechanism for the disclosed transformation, we were curious about the performance of more electron-rich substrates such as tetralin (**1h**), as these compounds may compete with $LiNO_3$ by reductively quenching **Xyl^F-Acr$^+$*** (Chart 2A). Owing to the extremely high acidity of the benzylic protons of arene radical cations,[39] one could envision an alternate mechanistic pathway where radical **1$^\bullet$** is formed through oxidation and deprotonation of **1**, obviating the need for $LiNO_3$ (Chart 2B). As expected, tetralin (**1h**) can be efficiently converted to 2-tetralone (**2h**), a challenging motif to access directly by traditional synthetic methods, without the use of $LiNO_3$ (Chart 2C). These conditions also allowed for lower [Co^{II}] loadings and shorter reaction times, further supporting our hypothesis that prolonged exposure of the cobaloxime to *in situ* generated HNO_3 likely leads to catalyst decomposition. These conditions also proved to be more functional group tolerant than those presented in Chart 1.

When selecting the appropriate conditions for this transformation, the redox properties of both the photocatalyst and substrate should be considered. As a general rule of thumb, if electron transfer is energetically favorable, the conditions without $LiNO_3$ should be employed. For example, **1a** was found by cyclic voltammetry to have a $E^{ox}_{p/2}$ of +2.27 V and is therefore not likely to undergo facile SET with **Xyl^F-Acr$^+$*** ($E^*_{red} = +2.13V$) and will require the use of $LiNO_3$ as a mediator. However, **1h** ($E^{ox}_{p/2} = +2.03V$) is poised to undergo thermodynamically favorable SET. Stern–Volmer analysis should be used to determine actual ability of a particular substrate to quench **Xyl^F-Acr$^+$***; however, CV analysis will allow for a reasonable approximation.

In conclusion, we have developed a protocol for the selective oxidation of traditionally unreactive C–H bonds. Experiments were performed to probe the mechanism of this dual-catalytic, two-part transformation, which guided efforts to devise separate sets of conditions to address differences associated with the electronic properties of individual substrates. An initial look into the substrate scope has revealed the potential utility of this reaction, which allows for the direct access of dissonant motifs from inexpensive and simple starting materials. Ongoing work is focused on refining this protocol for specific applications that we anticipate could make impacts in multiple facets of the chemical industry.

Supplementary Material

Refer to Web version on PubMed Central for supplementary material.

ACKNOWLEDGMENTS

Financial support was provided in part by the National Institutes of Health (NIGMS) Award No. R01 GM098340 and a Camille Dreyfus Teacher-Scholar Award. Photophysical measurements were performed in the AMPED EFRC Instrumentation Facility established by the Alliance for Molecular PhotoElectrode Design for Solar Fuels (AMPED), an Energy Frontier Research Center (EFRC) funded by the U.S. Department of Energy, Office of Science, Office of Basic Energy Sciences under Award DE-SC0001011. We thank the University of North Carolina's Department of Chemistry Mass Spectrometry Core Laboratory, especially Dr. Brandie Ehrmann, for

assistance with mass spectrometry analysis. We acknowledge Professor Thomas Meyer (UNC) for assistance in stopped-flow experimentation.

REFERENCES

(1). White MC; Zhao J Aliphatic C–H Oxidations for Late-Stage Functionalization. J. Am. Chem. Soc 2018, 140 (43), 13988–14009. [PubMed: 30185033]

(2). Meunier B; de Visser SP; Shaik S Mechanism of Oxidation Reactions Catalyzed by Cytochrome P450 Enzymes. Chem. Rev 2004, 104 (9), 3947–3980. [PubMed: 15352783]

(3). Fernandes RA; Nallasivam JL Catalytic Allylic Functionalization *via* π-Allyl Palladium Chemistry. Org. Biomol. Chem 2019, 17 (38), 8647–8672. [PubMed: 31553038]

(4). Blanksby SJ; Ellison GB Bond Dissociation Energies of Organic Molecules. Acc. Chem. Res 2003, 36 (4), 255–263. [PubMed: 12693923]

(5). Baran PS; Zhong Y-L Selective Oxidation at Carbon Adjacent to Aromatic Systems with IBX. J. Am. Chem. Soc 2001, 123 (13), 3183–3185. [PubMed: 11457049]

(6). Nicolaou KC; Montagnon T; Baran PS; Zhong Y-L Iodine(V) Reagents in Organic Synthesis. Part 4. o-Iodoxybenzoic Acid as a Chemospecific Tool for Single Electron Transfer-Based Oxidation Processes. J. Am. Chem. Soc 2002, 124 (10), 2245–2258. [PubMed: 11878978]

(7). Zhang W; Wang F; McCann SD; Wang D; Chen P; Stahl SS; Liu G Enantioselective Cyanation of Benzylic C–H Bonds via Copper-Catalyzed Radical Relay. Science 2016, 353 (6303), 1014–1018. [PubMed: 27701109]

(8). Lee BJ; DeGlopper KS; Yoon TP Site-Selective Alkoxylation of Benzylic C–H Bonds by Photoredox Catalysis. Angew. Chem., Int. Ed 2020, 59 (1), 197–202.

(9). Yamazaki S Chromium(VI) Oxide-Catalyzed Benzylic Oxidation with Periodic Acid. Org. Lett 1999, 1 (13), 2129–2132.

(10). Horn EJ; Rosen BR; Chen Y; Tang J; Chen K; Eastgate MD; Baran PS Scalable and Sustainable Electrochemical Allylic C–H Oxidation. Nature 2016, 533 (7601), 77–81. [PubMed: 27096371]

(11). D'Accolti L; Dinoi A; Fusco C; Russo A; Curci R Oxyfunctionalization of Non-Natural Targets by Dioxiranes. 5. Selective Oxidation of Hydrocarbons Bearing Cyclopropyl Moieties [1]. J. Org. Chem 2003, 68 (20), 7806–7810. [PubMed: 14510559]

(12). Mello R; Fiorentino M; Fusco C; Curci R Oxidations by Methyl(Trifluoromethy1)Dioxirane. 2. Oxyfunctionalization of Saturated Hydrocarbons. J. Am. Chem. Soc 1989, 111 (17), 6749–6757.

(13). Chen MS; White MC A Predictably Selective Aliphatic C H Oxidation Reaction for Complex Molecule Synthesis. Science 2007, 318 (5851), 783–787. [PubMed: 17975062]

(14). Chen MS; White MC Combined Effects on Selectivity in Fe-Catalyzed Methylene Oxidation. Science 2010, 327 (5965), 566–571. [PubMed: 20110502]

(15). Nanjo T; de Lucca EC; White MC Remote, Late-Stage Oxidation of Aliphatic C–H Bonds in Amide-Containing Molecules. J. Am. Chem. Soc 2017, 139 (41), 14586–14591. [PubMed: 28921954]

(16). Howell JM; Feng K; Clark JR; Trzepkowski LJ; White MC Remote Oxidation of Aliphatic C–H Bonds in Nitrogen-Containing Molecules. J. Am. Chem. Soc 2015, 137 (46), 14590–14593. [PubMed: 26536374]

(17). Osberger TJ; Rogness DC; Kohrt JT; Stepan AF; White MC Oxidative Diversification of Amino Acids and Peptides by Small-Molecule Iron Catalysis. Nature 2016, 537 (7619), 214–219. [PubMed: 27479323]

(18). Kawamata Y; Yan M; Liu Z; Bao D-H; Chen J; Starr JT; Baran PS Scalable, Electrochemical Oxidation of Unactivated C–H Bonds. J. Am. Chem. Soc 2017, 139 (22), 7448–7451. [PubMed: 28510449]

(19). Newhouse T; Baran PS If C-H Bonds Could Talk: Selective C-H Bond Oxidation. Angew. Chem., Int. Ed 2011, 50 (15), 3362–3374.

(20). Lyons TW; Sanford MS Palladium-Catalyzed Ligand-Directed C–H Functionalization Reactions. Chem. Rev 2010, 110 (2), 1147–1169. [PubMed: 20078038]

(21). Fuse H; Mitsunuma H; Kanai M Catalytic Acceptorless Dehydrogenation of Aliphatic Alcohols. J. Am. Chem. Soc 2020, 142 (9), 4493–4499. [PubMed: 32057240]

(22). Fuse H; Kojima M; Mitsunuma H; Kanai M Acceptorless Dehydrogenation of Hydrocarbons by Noble-Metal-Free Hybrid Catalyst System. Org. Lett 2018, 20 (7), 2042–2045. [PubMed: 29558157]

(23). Zhang G; Hu X; Chiang C-W; Yi H; Pei P; Singh AK; Lei A Anti-Markovnikov Oxidation of β-Alkyl Styrenes with H_2O as the Terminal Oxidant. J. Am. Chem. Soc 2016, 138 (37), 12037–12040. [PubMed: 27595272]

(24). Romero NA; Nicewicz DA Mechanistic Insight into the Photoredox Catalysis of Anti-Markovnikov Alkene Hydrofunctionalization Reactions. J. Am. Chem. Soc 2014, 136 (49), 17024–17035. [PubMed: 25390821]

(25). Margrey KA; Nicewicz DA A General Approach to Catalytic Alkene Anti-Markovnikov Hydrofunctionalization Reactions via Acridinium Photoredox Catalysis. Acc. Chem. Res 2016, 49 (9), 1997–2006. [PubMed: 27588818]

(26). Refer to SI for full details.

(27). Hering T; Slanina T; Hancock A; Wille U; König B Visible Light Photooxidation of Nitrate: The Dawn of a Nocturnal Radical. Chem. Commun 2015, 51 (30), 6568–6571.

(28). Dempsey JL; Brunschwig BS; Winkler JR; Gray HB Hydrogen Evolution Catalyzed by Cobaloximes. Acc. Chem. Res 2009, 42 (12), 1995–2004. [PubMed: 19928840]

(29). Dempsey JL; Winkler JR; Gray HB Kinetics of Electron Transfer Reactions of H_2 -Evolving Cobalt Diglyoxime Catalysts. J. Am. Chem. Soc 2010, 132 (3), 1060–1065. [PubMed: 20043639]

(30). Dempsey JL; Winkler JR; Gray HB Mechanism of H_2 Evolution from a Photogenerated Hydridocobaloxime. J. Am. Chem. Soc 2010, 132 (47), 16774–16776. [PubMed: 21067158]

(31). Blackmond DG Kinetic Profiling of Catalytic Organic Reactions as a Mechanistic Tool. J. Am. Chem. Soc 2015, 137 (34), 10852–10866. [PubMed: 26285166]

(32). All electrochemical potentials are reported against SCE.

(33). White A; Wang L; Nicewicz D Synthesis and Characterization of Acridinium Dyes for Photoredox Catalysis. Synlett 2019, 30 (07), 827–832.

(34). Cartwright KC; Tunge JA Decarboxylative Elimination of *N*-Acyl Amino Acids via Photoredox/Cobalt Dual Catalysis. ACS Catal. 2018, 8 (12), 11801–11806.

(35). Li G; Han A; Pulling ME; Estes DP; Norton JR Evidence for Formation of a Co–H Bond from $(H_2O)_2Co(DmgBF_2)_2$ under H_2: Application to Radical Cyclizations. J. Am. Chem. Soc 2012, 134 (36), 14662–14665. [PubMed: 22897586]

(36). Nguyen VT; Nguyen VD; Haug GC; Dang HT; Jin S; Li Z; Flores-Hansen C; Benavides BS; Arman HD; Larionov OV Alkene Synthesis by Photocatalytic Chemoenzymatically Compatible Dehydrodecarboxylation of Carboxylic Acids and Biomass. ACS Catal. 2019, 9 (10), 9485–9498.

(37). Cartwright KC; Davies AM; Tunge JA Cobaloxime-Catalyzed Hydrogen Evolution in Photoredox-Facilitated Small-Molecule Functionalization: Cobaloxime-Catalyzed Hydrogen Evolution in Photoredox-Facilitated Small-Molecule Functionalization. Eur. J. Org. Chem 2020, 2020 (10), 1245–1258.

(38). Wayner DDM; McPhee DJ; Griller D Oxidation and Reduction Potentials of Transient Free Radicals'. J. Am. Chem. Soc 1988, 110 (1), 132–137.

(39). Schmittel M; Burghart A Understanding Reactivity Patterns of Radical Cations. Angew. Chem., Int. Ed. Engl 1997, 36 (23), 2550–2589.

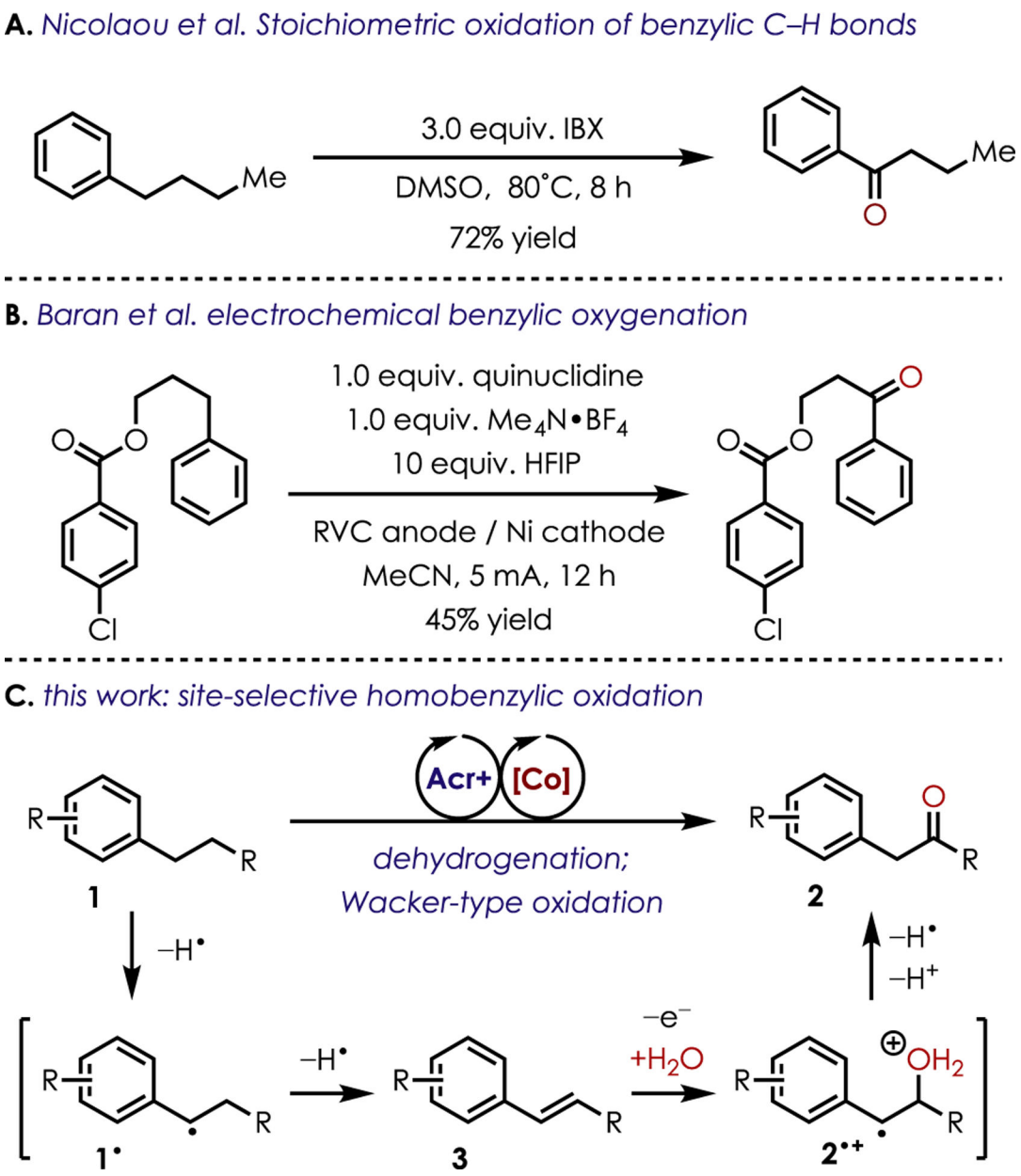

Figure 1.

(A, B) Traditional and state-of-the-art methods selective for benzylic oxidation. (C) Selective homobenzylic oxidation.

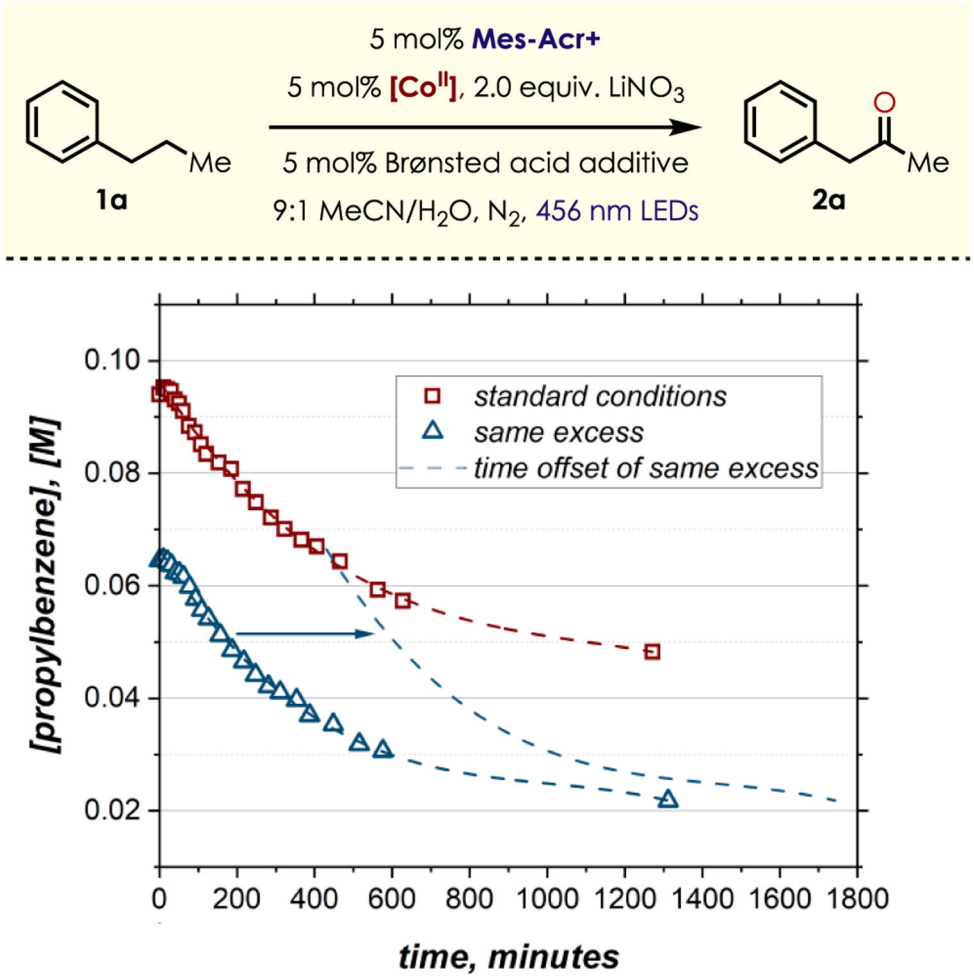

experiment	$[1a]_0$	$[H_2O]_0$	excess	$[2a]_0$
standard conditions	95 mM	5 M	4.91 M	–
same-excess + product	65 mM	5 M	4.94 M	30 mM

Figure 2.

Kinetic profile of **1a** oxidation under the HNO_3 conditions (red trace) and the same-excess experiment (blue trace).

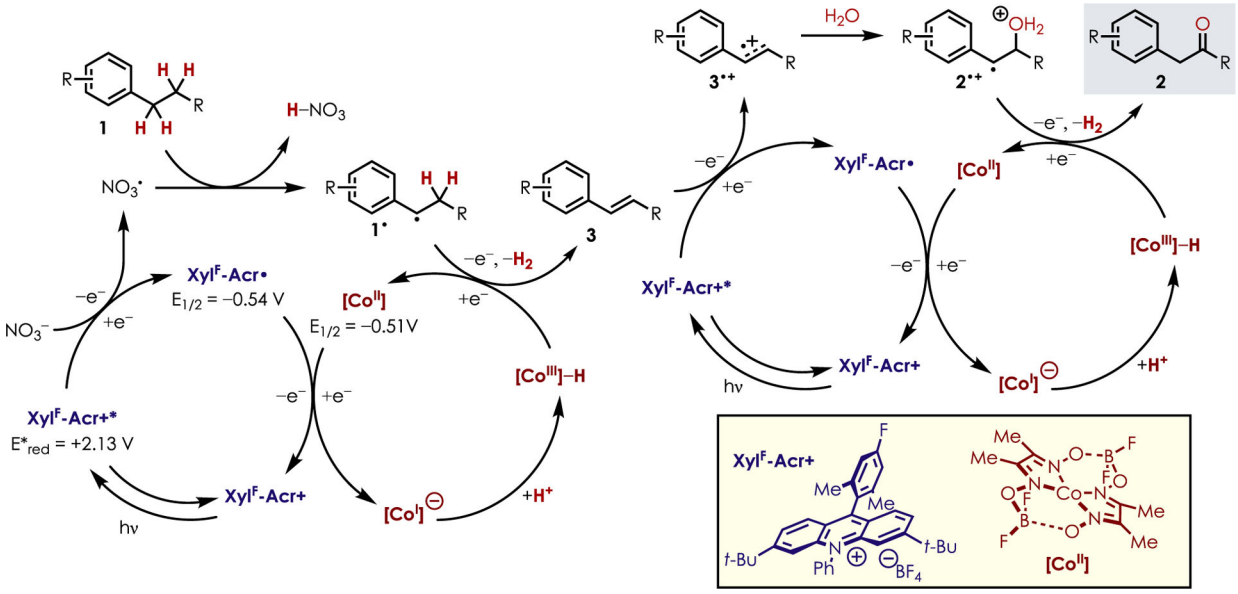

Scheme 1.

Mechanistic Proposal for $LiNO_3$-Mediated Homobenzylic Oxidation

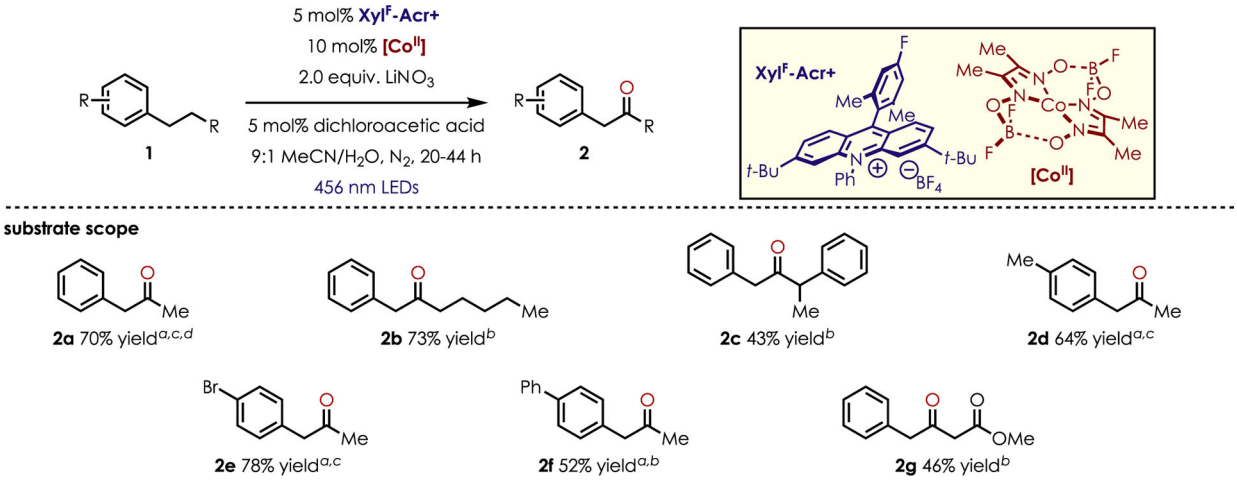

Chart 1.

Homobenzylic Oxidation Scope

[a]Yields determined by NMR vs an internal standard, [b]20 h. [c]44 h. [d]**Mes-Acr**$^+$ in place of **Xyl^F-Acr**$^+$.

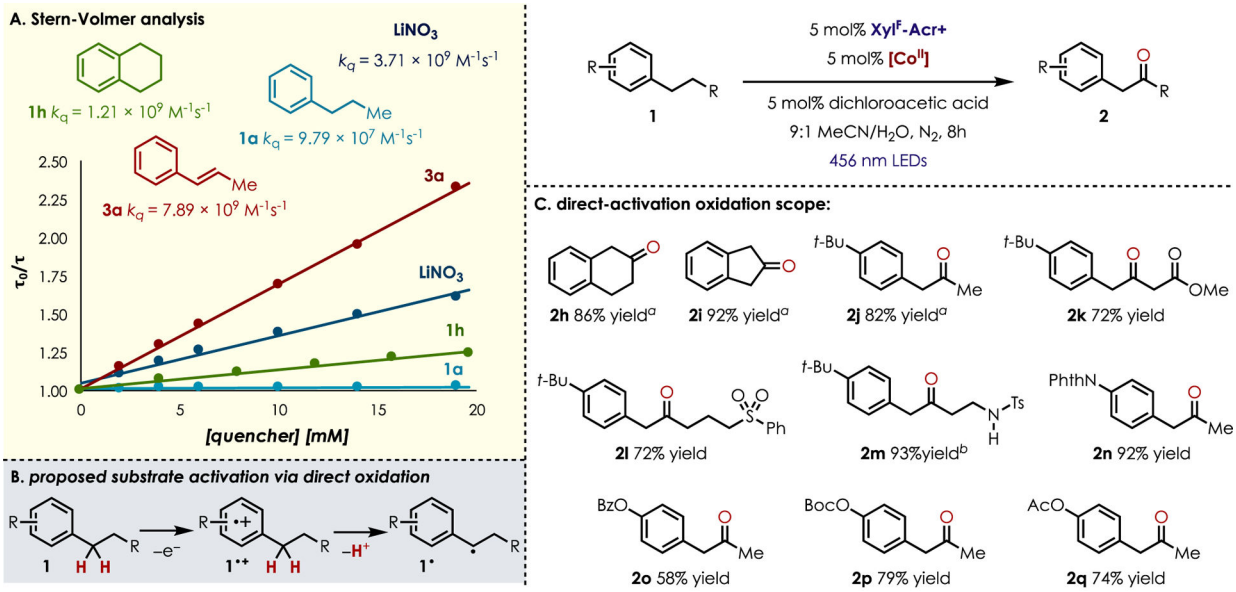

Chart 2.

(A) Stern–Volmer Analysis of Potential Quenching Molecules, (B) Proposal for Direct Substrate Oxidation Mechanism, and (C) Scope for Homobenzylic Oxidation

[a]Yields determined by NMR vs internal standard. [b]20 h. [c]44 h.

Table 1.

Optimization of Homobenzylic Oxidation

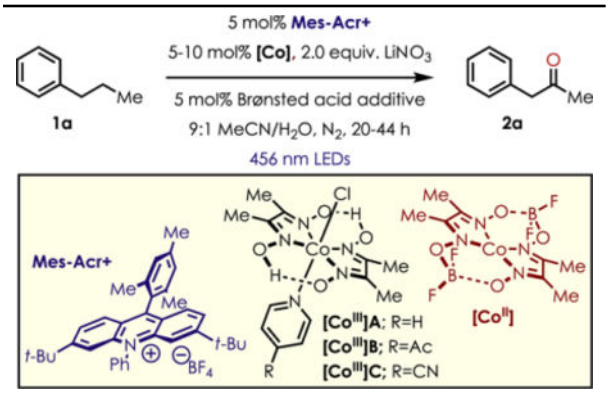

entry	[Co] source (mol %)	acid	yield (%)
1[a]	[Co^{III}]A (5)	–	22
2[a]	[Co^{m}]B (5)	–	11
3[a]	[Co^{m}]C (5)	–	4
4[a]	[Co^{n}] (5)	–	24
5[b]	[Co^{n}] (5)	HNO_3	55
6[b]	[Co^{n}] (5)	DCA	57
7[b]	[Co^{n}] (10)	HNO_3	55–74
8[b]	[Co^{n}] (10)	DCA	70
9[b,c]	[Co^{n}] (10)	DCA	trace

[a] 20 h reaction time.

[b] 44 h reaction time.

[c] 0 equiv $LiNO_3$. DCA = dichloroacetic acid. Yields were determined by NMR against HMDSO as an internal standard.